Article

Electrochemical Detection of *Borrelia burgdorferi* Using a Biomimetic Flow Cell System

Connor D. Flynn,* Mariusz Sandomierski, Kelly Kim, Julie Lewis, Vett Lloyd, and Anna Ignaszak*

Cite This: *ACS Meas. Sci. Au* 2023, 3, 208–216

Read Online

ACCESS | Metrics & More | Article Recommendations | Supporting Information

ABSTRACT: Lyme disease, caused by infection with pathogenic *Borrelia* bacteria, has emerged as a pervasive illness throughout North America and many other regions of the world in recent years, owing in part to climate-mediated habitat expansion of the tick vectors. Standard diagnostic testing has remained largely unchanged over the past several decades and is indirect, relying on detection of antibodies against the *Borrelia* pathogen, rather than detection of the pathogen itself. The development of new rapid, point-of-care tests for Lyme disease that directly detects the pathogen could drastically improve patient health by enabling faster and more frequent testing that could better inform patient treatment. Here, we describe a proof-of-concept electrochemical sensing approach to the detection of the Lyme disease-causing bacteria, which utilizes a biomimetic electrode to interact with the *Borrelia* bacteria that induce impedance alterations. In addition, the catch-bond mechanism between bacterial BBK32 protein and human fibronectin protein, which exhibits improved bond strength with increased tensile force, is tested within an electrochemical injection flow-cell to achieve *Borrelia* detection under shear stress.
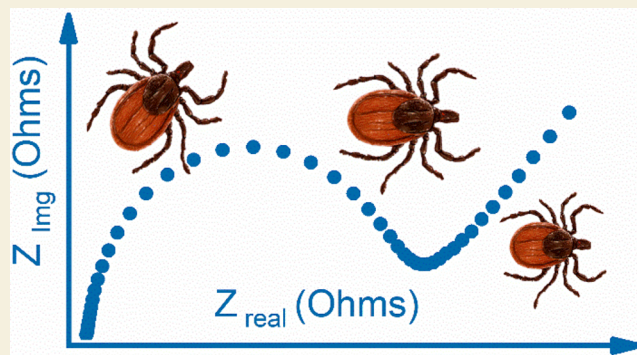
KEYWORDS: *Lyme disease, Borrelia, Biomimetic, Electrochemical impedance spectroscopy, Early detection*

INTRODUCTION

Lyme disease, or Lyme borreliosis, a term which indicates the causative agent, is the most prevalent tickborne illness in both North America and Europe, with an estimated 470,000 cases diagnosed each year in the United States alone.[1,2] Lyme disease can be caused by several pathogenic bacterial species within the *Borrelia* genus, but *Borrelia burgdorferi* is the primary infectious agent within North America. These bacteria are spread by ticks of the *Ixodes* genus, hard-bodied ticks common to many temperate regions of the world. The pervasiveness of Lyme disease has seen substantial increases in recent years owing to climate change-mediated tick migration, among other factors, with notable rises in cases across North America, Europe, and regions of Asia.[3−5] This increase in incidence of Lyme disease, coupled with the challenges that often accompany its rapid and accurate diagnosis, have driven significant interest in improving Lyme disease diagnostic capabilities.[6]

After transmission of Lyme bacteria into a host's body, the individual is at risk of developing Lyme disease.[7] While the bacteria initially remain at the site of infection, over time they begin to disseminate through the body to different tissues and organs, where they can reside and cause various health difficulties.[8] The stabilization of the *Borrelia* spirochetes within the body is achieved through the interaction of specific bacterial membrane proteins with human proteins found throughout the body. While *Borrelia* species express several adhesins that interact with human cells, the interaction between the *Borrelia* BBK32 protein and human fibronectin is particularly important for attachment.[9]

BBK32 is one of several known microbial surface components recognizing adhesive matrix molecules (MSCRAMMs) that mediate the attachment of *Borrelia* to host tissues.[10] Fibronectin, to which BBK32 adheres, is a 440 kDa glycoprotein dimer that exists throughout the body as both a soluble plasma protein and insoluble cellular protein.[11] Each fibronectin chain consists of 3 types of repeating domains: 12 fibronectin 1 (Fn-1) domains, 2 fibronectin 2 (Fn-2) domains, and 15−17 fibronectin 3 (Fn-3) domains. Fibronectin dimerization occurs through self-association between Fn-1 and Fn-3 domains.[12] Plasma fibronectin is also known to undergo additional association beyond dimerization to form large multimeric complexes, however, the mechanism behind this association is poorly understood.[13] BBK32 adheres to fibronectin through β-strand addition between the BBK32
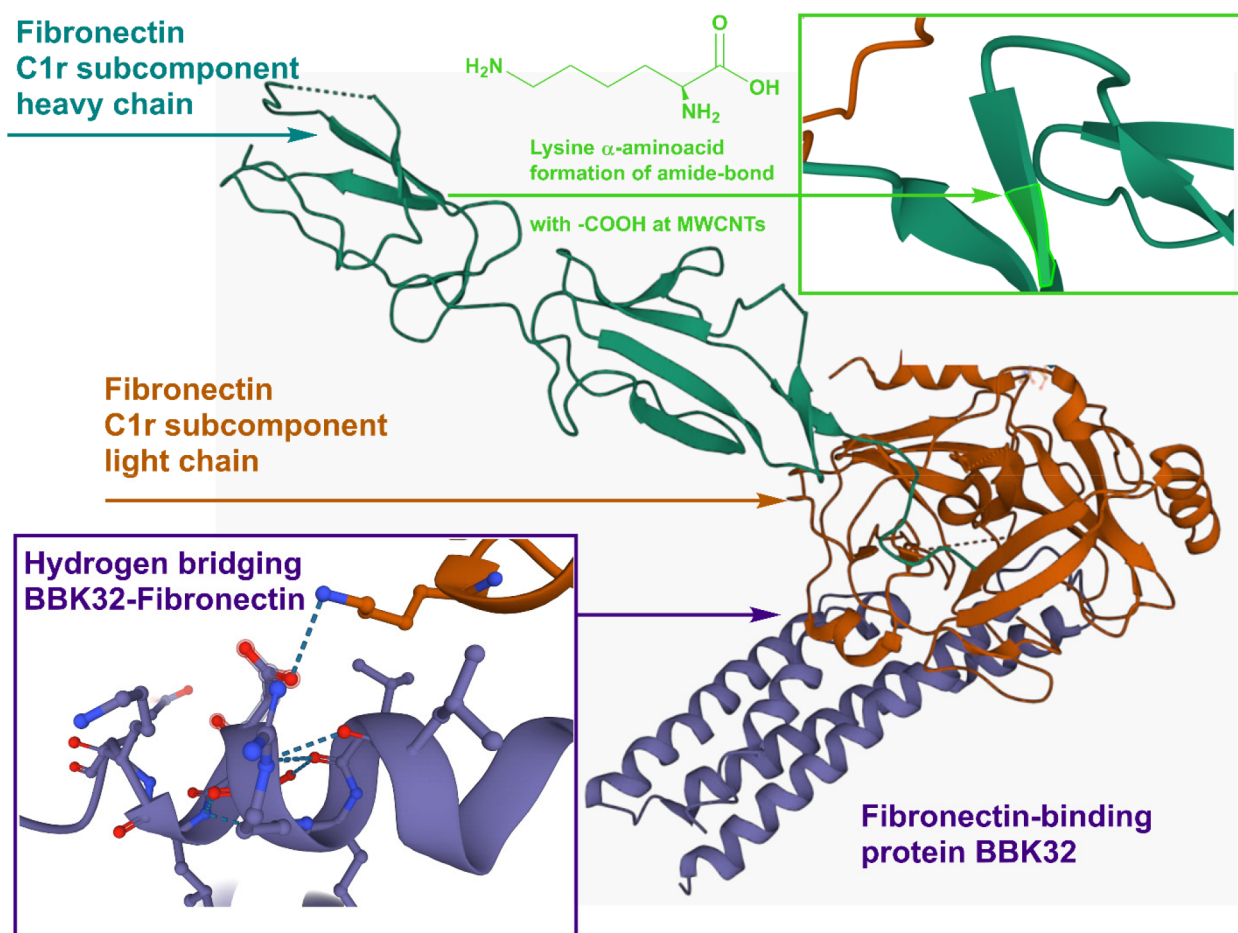
Figure 1. *Borrelia* BBK32 interaction with human fibronectin. BBK32 fragment (purple) binding to fibronectin C1r subcomponent light chain (orange), with a lysine amino acid (light green) projected in the C1r heavy chain of fibronectin (dark green) visualized using 3D Protein Feature View tools available from RCSB PDB Protein data Bank rcsb.org (RCSB PDB ID 7MZT), reported by Garrigues et al. using XRD data.[19]

N-terminal region and fibronectin Fn-1 domains.[14] This type of interaction involves the formation of a tandem β-zipper, where β-strands on both proteins adhere through hydrogen bonding in an antiparallel manner.[15] Evolutionary analysis of the BBK32 protein sequence (Figure S1) suggests it is vital to bacterial survival and thus makes an excellent target for detection.

Recent years have seen the emergence of several Lyme disease biosensing approaches;[6,16–18] however, while these devices provide promising diagnostic alternatives, the existence of an inexpensive and rapid test remains an unmet need. In response to this opportunity, the current study explores the potential of an electrochemistry-mediated biosensor for *Borrelia*, as a tool to help prevent the burden of Lyme disease associated with late detection. The biosensing methodology presented here is based on the well-established interaction between *Borrelia* BBK32 and human fibronectin proteins. Through functionalization of carbon screen-printed electrodes with fibronectin, a biomimetic surface that can interact with the BBK32 protein and, by extension, *Borrelia*, the Lyme disease-causing bacteria is produced. X-ray diffraction (XRD) data of the BBK32-fibronectin interaction,[19] as well as the relevant protein residues for the sensing mechanism, have been rendered as a 3-D model by Garrigues and colleagues,[19] as presented in Figure 1. Upon attachment of either *Borrelia* BBK32 or the entire bacterial cell to the electrode surface,

electrochemical measurements can provide a fast and quantifiable response to indicate bacterial presence.

■ EXPERIMENTAL SECTION

Materials and Methods

Multiwalled carbon nanotubes (MWCNTs), 1-ethyl-3-(3-(dimethylamino)propyl) carbodiimide (EDC), *N*-hydroxysuccinimide (NHS), potassium ferricyanide, potassium ferrocyanide, potassium chloride, disodium phosphate, trisodium phosphate, and nitric acid were purchased from MilliporeSigma (Canada). Human plasma fibronectin purified protein in 150 mM sodium chloride and 10 mM sodium phosphate (pH = 7.5) was obtained from MilliporeSigma (Canada). StartingBlock (PBS) blocking buffer was obtained from Thermo Fisher Scientific (Canada). TOP-10 *Escherichia coli* was supplied by courtesy of Dr. Yang Qu at the University of New Brunswick. All chemical solids used during experimentation were measured using Mettler Toledo balances. All electrochemical measurements were carried out using CHI660E and CHI760E potentiostats, purchased from CH Instrumentation (USA). Carbon screen-printed electrodes (SPEs) were obtained from Pine Research Instrumentation (USA). Carboxyl-functionalized MWCNT-coated carbon SPEs were acquired from Metrohm DropSens (cat. 110CNT) for use in a flow-cell format. The electrochemical flow cell (model DRP-CFLWCL-MAGN) was purchased from Metrohm Canada and connected to a peristaltic pump (model MasterFlex L/S) from Cole-Parmer (USA).

MWCNT Oxidation

MWCNTs were oxidized to introduce carboxylic acid functionalities to their surfaces. MWCNT oxidation was achieved through reflux in nitric acid using a protocol adapted from Rosca et al.[20] Approximately 0.35 g of MWCNTs was dispersed in 60% nitric acid at a concentration of 7 mg/mL and refluxed for 18 h at 118 °C. Upon reflux completion, the MWCNT mixture was vacuum filtered and thoroughly rinsed with distilled water to ensure removal of small carbon fragments and other impurities. The purified MWCNT powder was oven-dried for 24 h at 50 °C.

MWCNT oxidation was confirmed using X-ray photoelectron spectroscopy (XPS) to characterize the nature of carbon and oxygen atoms present within the sample. All XPS experiments were performed using a VG Microtech MultiLab ESCA 2000 X-ray photoelectron spectrometer at Dalhousie University. The integrity of oxidized MWCNT was confirmed using a JEOL JEM 2011 scanning transmission electron microscope (STEM) at the University of New Brunswick.

Electrode Functionalization of Bare SPEs

Carbon screen-printed electrodes (unmodified) were activated/cleaned prior to use by exposure of the working electrode to concentrated nitric acid for 5 min, followed by thorough rinsing with distilled water. After activation of the SPEs, oxidized MWCNTs were drop-casted onto the working electrode surface. MWCNTs were diluted in distilled water to a stock concentration of 0.5 mg/mL, and 5 μL of this MWCNT solution was deposited onto the working electrode. The SPEs were dried at room temperature for approximately 45 min, until the MWCNT layer was dry and appeared as a smooth, uniform film. After formation of the MWCNT layer, the SPEs were rinsed with distilled water to remove any loosely attached MWCNTs and redried.

SPE functionalization began with the addition of cross-linking agents to prime the carboxylic acids for protein addition, using an adapted protocol.[21] A solution of 5 mM NHS and 2 mM EDC was drop-casted onto the MWCNT-coated working electrode; the SPE was then incubated for 60 min at 4 °C. After this incubation, the NHS/EDC solution was rinsed off with distilled water and 5 μL of a 1 mg/mL plasma fibronectin solution was immediately drop-casted onto the working electrode. The fibronectin solution was incubated on the electrodes for 60 min at 4 °C. After the fibronectin incubation, the electrodes were rinsed and incubated in 0.25× StartingBlock for 30 min. Following this final blocking step, electrodes were rinsed with distilled water and stored at 4 °C in ambient air. All incubations took place in a humidity chamber to minimize evaporation.

Premodified MWCNT carbon SPEs used for flow-cell analysis were prepared in an identical manner to the bare carbon SPEs, with the exception of the initial activation and MWCNT deposition steps.

Confirmation of Fibronectin Attachment

Attenuated total reflectance Fourier transform infrared spectroscopy (ATR-FTIR) was employed to confirm the presence of fibronectin proteins on the surface of the electrode. All ATR-FTIR experiments were carried out with a Bruker Alpha II FTIR spectrometer with an accompanying ATR-FTIR attachment. Scanning electron microscopy (SEM) was also employed to visualize the SPE surface following fibronectin functionalization.

Borrelia Bacteria Samples

All *Borrelia* samples (*B. burgdorferi* strain: ATCC 35210) were cultured in the modified Barbour-Stoenner-Kelly medium, BSK-H, with 6% rabbit serum[22] (Dalynn Biologicals) with antibiotics (amphotericin B at 2.5 μg/mL, rifampicin at 0.05 mg/mL, and phosphomycin at 0.02 mg/mL) from Sigma-Aldrich, for at least 4 weeks at 34−35 °C with 5% CO_2. *Borrelia* cells were killed by exposure to a dilute salt environment (0.1× PBS) and freezing for >48 h at −80 °C. *Borrelia* cell extracts were stored at −20 °C until use.

The incubation of fibronectin-modified electrodes in analytes involved drop-casting of the *Borrelia* samples onto the electrode surface and subsequent incubation in a humidity chamber. After

analyte incubation, electrodes were rinsed with distilled water prior to electrochemical measurement.

E. coli was chosen as a negative control in all electrochemical tests due to similarity in the size of species (*B. burgdorferi* that is approximately 0.3 μm wide and 5−20 μm long and the *E. coli* with approximately 1.1−1.5 μm wide and 2−6 μm long).

Microscopy Analysis

SEM images were obtained using a JEOL JSM 6400 scanning electron microscope, after sputter coating of samples with an ultrathin layer of gold. Bacteria-coated electrodes were dried out prior to imaging and stored at −20 °C until imaging, which was performed within 24 h of electrode incubation.

Electrochemical Analysis

Electrochemical impedance spectroscopy (EIS) and cyclic voltammetry (CV) measurements were performed in a cell solution containing 10 mM phosphate buffer, 50 mM potassium chloride, and 5 mM ferrocyanide/ferricyanide (pH = 7.4). Electrodes were interrogated with protein/bacteria via horizontal incubation in a humidity chamber, followed by thorough rinsing in cell solution prior to analysis. All measurements took place in a vertical electrochemical cell. The open-circuit potential (OCP) was recorded for 10 min prior to any electrochemical measurement to ensure electrode stability. All EIS data collected for the *Borrelia* sensor used an applied AC amplitude of 5 mV, a frequency range of 0.1−1 000 000 Hz, and an applied potential equal to OCP.

Impedimetric Flow Cell Analysis

The electrochemical flow cell suitable for Drop Sense SPE electrodes was connected to a peristaltic pump (Figure S2). The flow rate of the circulating solution was set based on two assumptions: (1) the catch-bond force facilitating the interaction between human fibronectin and Lyme bacteria occurs as the bacteria move over endothelial surfaces with a velocity of approximately 100 μm/s;[23] for this reason, tubing with an internal diameter of 0.8 mm and a cross-sectional area of 0.50265 mm^2 was selected to enable a flow rate as low as 0.003 mL/min—a linear velocity of 100 μm/s; and (2) the flow rate of human blood is 3−26 mL/min in arteries and 1.2−4.8 mL/min in veins;[24] therefore, in order to mimic this catch bond environment, the flow rate of the measurement buffer containing an appropriate amount of analyte target species was set at 0.06, 0.125, 0.5, 1, and 2 mL/min. The Lyme bacteria and control bacteria (*E. coli*) were injected in the circulating buffer at final concentrations of 0, 500, 1000, and 2000 cells/mL. All flow tests were carried out in the same cell solution used for the EIS experiments. OCP was recorded for 10 min prior to any electrochemical measurement to ensure electrode stability. Single frequency impedance was recorded at 1000 Hz at OCP for 7200 s with a 20 s sampling period for carbon SPEs mounted in the electrochemical flow cell. The chemical composition of circulating solution was 10 mM phosphate buffer and 50 mM potassium chloride (pH = 7.4) and the whole Lyme bacteria and *E. coli* extracts were added to the circulating solution.

■ RESULTS AND DISCUSSION

MWCNT Oxidation and Electrode Functionalization

MWCNTs were oxidized to introduce carboxylic acid functionalities for subsequent protein attachment. MWCNT oxidation was confirmed and characterized with XPS. Analysis of the carbon XPS spectra (Figure S3a) showed evidence of carboxylic acid functionalization. The peaks at ~286 and ~288 eV correspond to the presence of hydroxyl and carbonyl groups, respectively. These peaks were not present to a significant degree in the carbon XPS spectra of commercially acquired nonoxidized MWCNTs (Figure S3a, inset), pointing toward their development during the oxidation process. Specifically, these two functionalities exist within carboxylic acids and suggest the presence of said functional groups.

XPS analysis was also used to explore the oxygen spectra of the oxidized MWCNT (Figure S3b). The peak at ~531 eV corresponds to carboxylic acid functionalities and provides direct evidence of successful oxidation. The oxygen XPS spectrum of the nonoxidized MWCNTs (Figure S3b, inset) showed no evidence of carboxylic acid formation.

Since the oxidation of MWCNT used relatively harsh conditions, and because long exposure to nitric acid is known to degrade carbon nanotubes,[20] MWCNT were assessed for potential breakdown after the acid treatment. TEM was used to visualize the MWCNT before and after the oxidation process (Figure S3c). The long, filamentous nanotubes appear to be roughly the same shape and size in both images, suggesting that there was no significant damage caused by the nitric acid treatment.

SEM was employed in an attempt to visualize the fibronectin proteins bound to the MWCNTs. According to previous work on fibronectin morphology, plasma fibronectin exists as long filamentous proteins (up to a few μm in length) of approximately 2−3 nm diameter after refrigeration at 4 °C.[25] However, fibronectin is known to have a very dynamic structure and can exist in many different shapes and sizes, including both an elongated and compact form.[26] SEM of the fibronectin-MWCNT-modified electrodes (Figure 2) showed
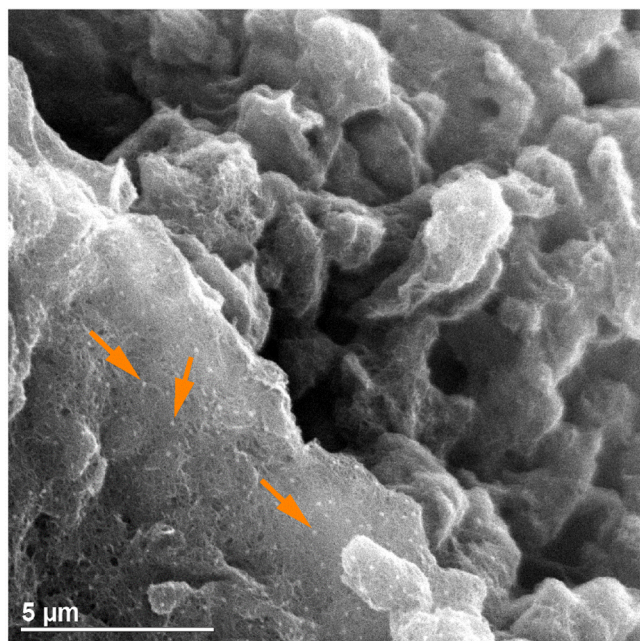
Figure 2. SEM visualization of fibronectin on MWCNT. SEM image of fibronectin modified MWCNT attached to carbon SPEs. The arrows highlight some of the small white structures that presumably represent clumps of fibronectin.

small, white amorphous shapes distributed uniformly across the MWCNT surface. The white structures were roughly 100−120 nm in diameter. While the 100−120 nm diameter visual estimate from SEM is significantly different than the 2−3 nm estimate predicted from the literature, it is not unexpected. Fibronectin is well-documented to undergo polymerization in the presence of metal ions, polyamines, and other unknown factors.[27,28] Thus, the white structures are likely multiple fibronectin molecules associated with one another; this also explains the apparent difference in their sizes as each may

possess a variable number of individual proteins. It is also likely that there are smaller, less-polymerized fibronectin groups present, but these are outside the resolution of the instrument.

SPE functionalization was assessed at each step of the modification process to ensure the expected alterations in electrochemical measurement were observed. In general, any modification that increased the surface conductivity of the electrode was expected to increase measured current and enhance charge-transfer. Likewise, any modification that obstructed the electrode surface was expected to decrease measured current and impede charge-transfer. The activity of the electrode was assessed using both EIS (Figure 3a) and CV (Figure 3b) in the presence of ferricyanide/ferrocyanide. Initially, the bare carbon SPE, prior to any modification, exhibited a low peak oxidation current (100 μA) and the highest charge-transfer resistance (R_{CT}, 9100 Ω), compared to subsequent modification steps. This observation is consistent with the expected low activity of the bare SPE, prior to nitric acid activation. According to the manufacturer, the factory produced SPEs contain surface binding agents and other contaminants that initially impede the electrode's activity.

Next, the nitric acid treatment was applied to activate the electrode and enhance kinetics. The CV (Figure 3b) shows a significant improvement in peak oxidation current (130 μA) after the activation. Similarly, the EIS spectrum shows a significant decrease in R_{CT}, moving from 9100 to approximately 500 Ω. Electrode activation was followed by MWCNT deposition, which was expected to significantly increase the conductivity of the electrode surface. CV of the MWCNT-modified electrode (Figure 3b) showed an increase in peak oxidation current (142 μA) relative to the electrodes without MWCNTs, as expected. The R_{CT} also decreased (~450 Ω) relative to the nitric acid treatment (Figure 3a); however, this decrease was very small compared to other R_{CT} alterations.

Fibronectin functionalization involved the attachment of proteins to the surface of the working electrode. These proteins were expected to block the electrode surface and also repel the redox probe at physiological pH due to the protein's lower isoelectric point.[29] CV of the fibronectin-modified electrode (Figure 3b) showed a large decrease in measured peak oxidation current (92 μA), which was lower than the initial bare electrode. EIS (Figure 3a) also showed a large increase in R_{CT}, which changed from approximately 500 to 2500 Ω.

Bacterial Adherence to Modified Electrodes

SEM images were collected for both fibronectin-free and fibronectin-functionalized MWCNT-modified SPEs (Figure 4). These electrodes were exposed to a 2500 cells/mL solution of dead *B. burgdorferi* cells for 30 min prior to imaging. While the control electrode (Figure 4a), without fibronectin, showed no evidence of bacterial attachment, the fibronectin-functionalized electrode (Figure 4b) exhibited amorphous shapes distributed over the surface. These forms were translucent and appeared in a variety of shapes, all relatively compact.

The observed forms were not long and thin as expected of spirochetes during vegetative growth, but *Borrelia* are well-known to be pleomorphic; under hostile environmental conditions or nutrient depletion, they adopt nonspirochaetal morphologies, many spherical.[30−36] These forms may have been the result of freezing the cells or preparation of the cells for scanning electron microscopy. The putative *B. burgdorferi* cells on the electrode surface measured approximately 400−
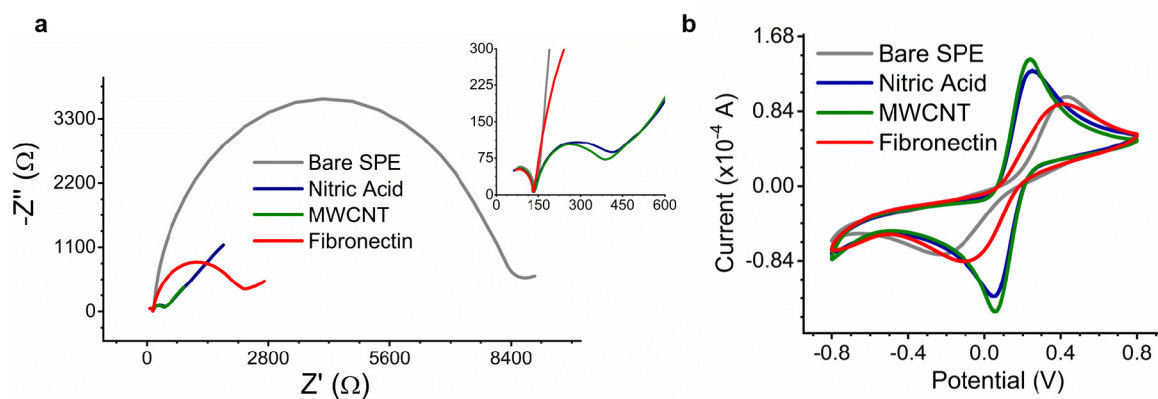
Figure 3. Electrochemical characterization of functionalized electrodes. (a) EIS Nyquist plots and (b) CVs recorded at each step of the fibronectin functionalization process, including the bare SPEs, nitric acid activation, MWCNT deposition, and fibronectin attachment.
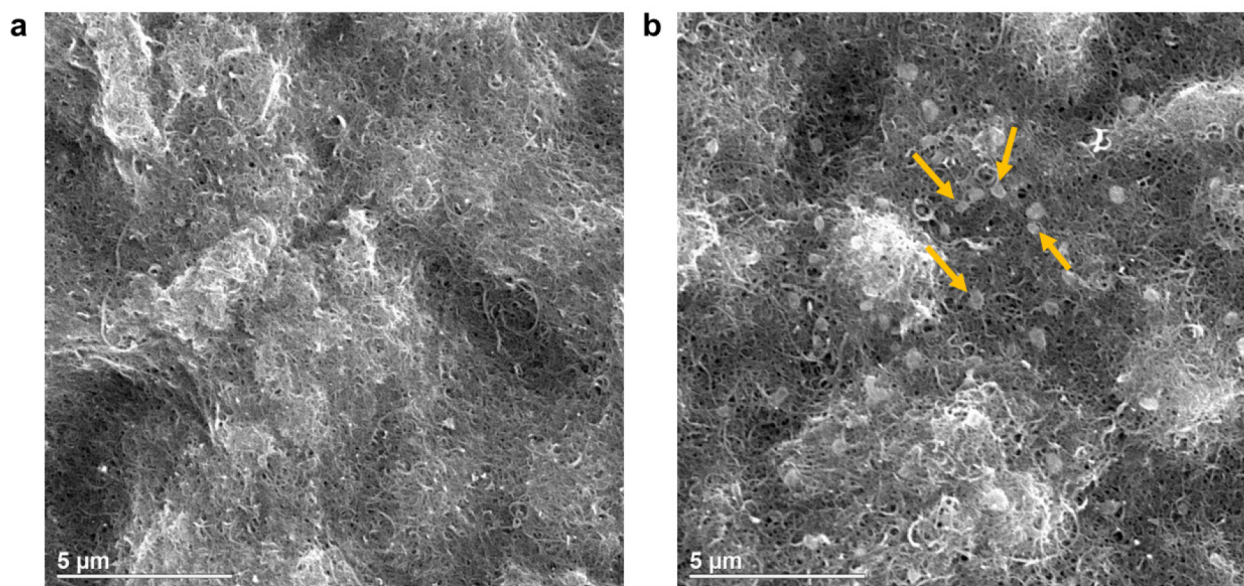
Figure 4. SEM images of *Borrelia*-incubated electrodes. (a) Fibronectin-free and (b) fibronectin-functionalized MWCNT-modified SPE after exposure to 2500 cells/mL *B. burgdorferi* bacteria extract for 30 min.

500 nm in diameter. This observed length is consistent with the sizes described for *B. burgdorferi* round-body forms.[30−36]

Impedimetric Detection of Lyme Bacteria

Electrochemical detection of *B. burgdorferi* bacteria was achieved using faradaic EIS in the presence of the ferricyanide/ferrocyanide redox couple. The electrochemical interface, consisting of the MWCNT scaffold, the fibronectin recognition element, and the adhered *Borrelia* bacteria, as well as the estimated equivalent circuit for this system, are depicted in Figure 5. Upon association of the *B. burgdorferi* bacteria with the fibronectin, steric blockage of the electrode surface led to reduced redox interchange, observed through increases in R_{CT} and modulation of surface capacitance.

Electrochemical analysis of the fibronectin-functionalized electrodes was conducted to determine whether *B. burgdorferi* cells adhered to the sensor surface. EIS was performed both before and after bacterial incubation, with bacterial attachment expected to increase R_{CT} through increased electrode coverage. Initial EIS analysis of *B. burgdorferi* exposed to fibronectin electrodes showed a significant increase in R_{CT} of around 1000 Ω after 30 min exposure to the *Borrelia* bacteria (Figure 6a).

Subsequent exposure of fibronectin SPEs to *E. coli* bacteria, a control bacteria used to examine specificity, showed no noticeable change in R_{CT} after 30 min of incubation (Figure 6b).

Further EIS analysis of *B. burgdorferi* bacteria at various concentrations revealed a corresponding increase in R_{CT} upon increased bacterial exposure (Figure 7a), determined using the equivalent circuit fit (Figure 7b). This increase in R_{CT} appeared to scale linearly with bacterial concentration in the tested range between 0 and 3666 cells/mL (Figure 7c). From the obtained data, the sensor is estimated to have a limit of detection of approximately 200 cells/mL. The experimental LOD of 200 cells/mL (± 15%) is stated based on observation, revealing that a consistent change in the sensor response took place at the concentration of Lyme extract that was higher than 200 cells/mL in almost every trial.

Flow Cell Analysis of *B. burgdorferi* Attachment

In order to interact with the endothelial lining of blood vessels, which is critical for the progression of the infectious disease, *B. burgdorferi* must overcome the shear stress due to blood flow through specific interactions with proteins in the blood, lymph,
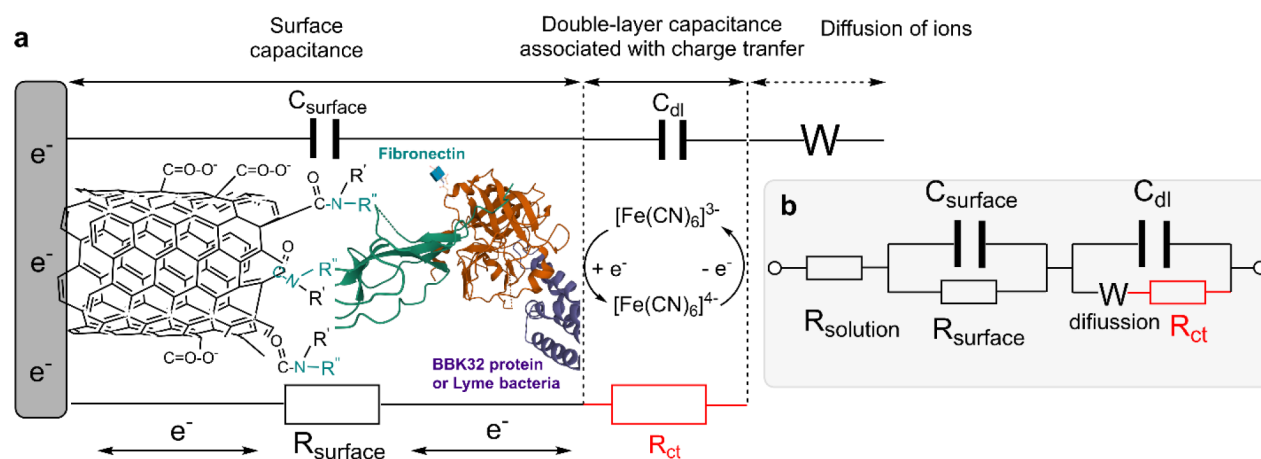
Figure 5. Schematic for the electrochemical detection mechanism of *Borrelia*. (a) Formation of an electrochemical signal (impedance and Faradaic current) in the Lyme-bacteria sensor composed of fibronectin-coated MWCNT SPEs; the bridging between fibronectin and MWCNT is achieved via an amide-like linker, formed between carboxyl groups present on the carbon surface and free amine groups of fibronectin; electron (e^-) transfer due to redox reaction involving $[Fe(CN)_6]^{3-}/[Fe(CN)_6]^{4-}$ mediator is marked as reverse arrows at the bottom. The structure of the fibronectin-BBK32 affinity is generated based on projections from Figure 1 using Protein Feature View tools available from RCSB PDB Protein data Bank (RCSB PDB ID 7MZT) reported by Garrigues et al. on reported XRD data.[19] (b) Electrical equivalent circuit used for fitting of impedance spectra, allowing us to identify resistance and capacitance at the sensor interface.
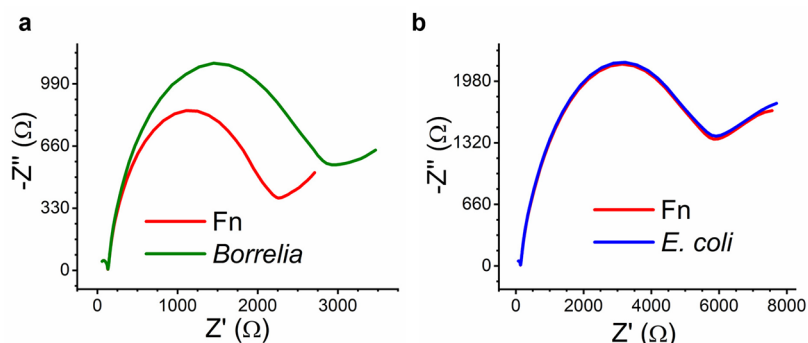
Figure 6. Interrogation of fibronectin-MWCNT SPEs with bacteria. (a) EIS curves of modified electrode exposed to 2000 cells/mL *B. burgdorferi* bacteria for 30 min. (b) EIS curves of modified electrode exposed to 2000 cells/mL *E. coli* for 30 min.
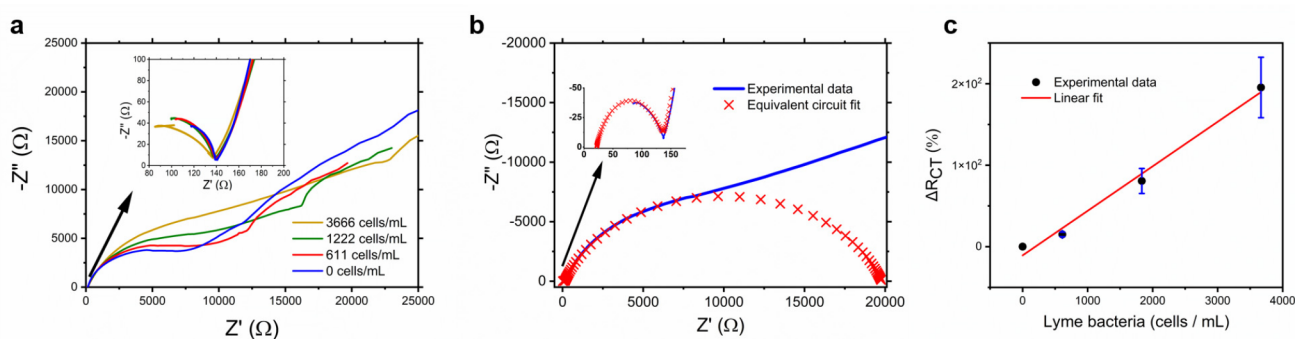
Figure 7. Impedimetric detection of *B. burgdorferi*. (a) Observed trend in Nyquist curves for fibronectin modified MWCNT SPE with increasing concentrations of *B. burgdorferi*. (b) Equivalent circuit fit for the obtained EIS data as shown in Figure 5b. (c) Calibration curve of *B. burgdorferi* detection, showing the obtained linear fit (*n* = 2).

and endothelial cells.[37] The interaction between *B. burgdorferi* BBK32 and fibronectin occurs via a catch bond—a noncovalent interaction whose strength increases with tensile strength.[23] A thorough analysis of the biomechanical mechanism by which fibronectin promotes the catch-bond between vascular surface and the BBK32 adhesin has been reported previously by Ebady and colleagues in 2016.[37] It has been demonstrated that

bacteria utilize the force generated by blood movement to adhere to endothelial tissue, using processes that are similar to the mechanisms facilitating leukocyte movement over vascular walls. Furthermore, it has been suggested that under physiological shear stress, pockets of polymerized plasma fibronectin at bacterial poles create adhesion complexes; polymerized fibronectin strengthens and stabilizes these
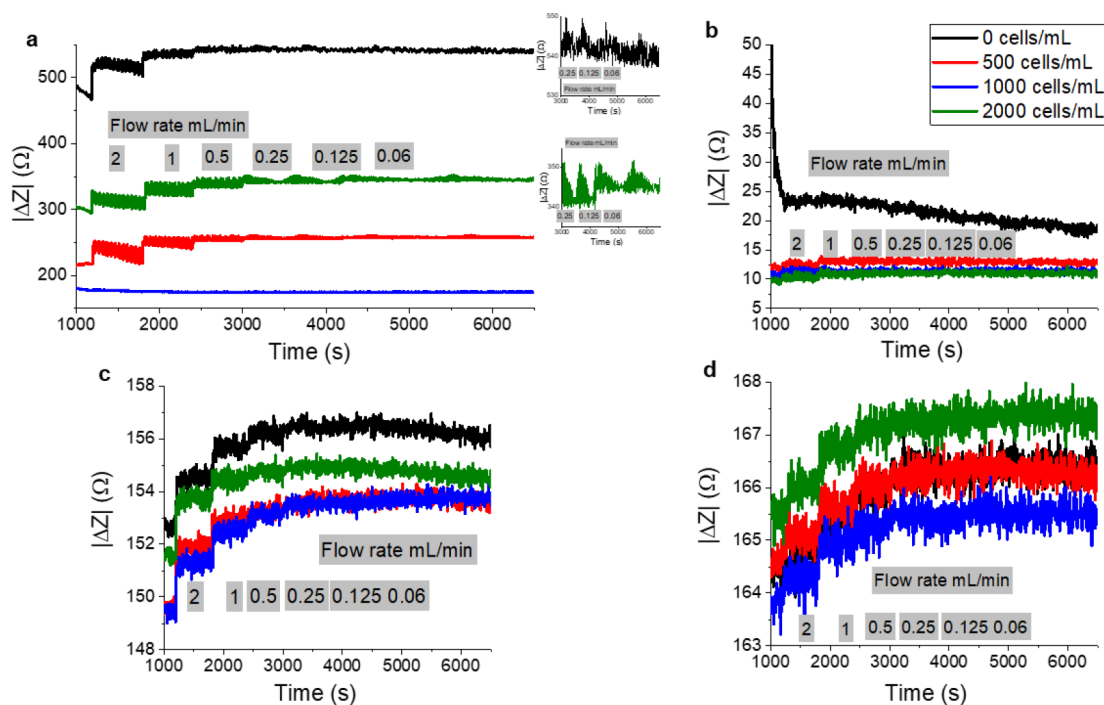
Figure 8. Impedimetric flow cell analysis of bacteria−SPE interactions. Observed impedance changes of carbon electrode mounted in a flow-injection electrochemical cell for (a) a fibronectin-modified electrode exposed to 0−2000 cells/mL of *B. burgdorferi* bacteria, (b) a bare electrode exposed to 0−2000 cells/mL of *B. burgdorferi*, (c) a fibronectin-modified electrode exposed to 0−2000 cells/mL of *E. coli* bacteria, and (d) a bare electrode exposed to 0−2000 cells/mL of *E. coli* bacteria.

interactions via a catch-bond mechanism. These results have shown that *B. burgdorferi* can transform normally nonadhesive blood components to increase the strength and stability of bacterial interactions with vascular surfaces. To better assess whether the fibronectin-*Borrelia* catch-bond mechanism could be captured by the present electrochemical system, the modified electrodes were tested under flow conditions mimicking those found in the human body.

To determine whether flow rate can affect the shear-force induced interaction between the target *B. burgdorferi* and the fibronectin immobilized onto the sensor, we examined the total change in impedance of the electrode upon a variable flow rate for fibronectin-modified electrodes and bare electrodes tested against both *B. burgdorferi* and *E. coli* bacteria. Upon addition of *B. burgdorferi* to the sensors (Figure 8a,b), there is a significant difference in the absolute change of impedance for the fibronectin-modified electrodes. These differences span over 150−300 Ω with increasing content of circulating *B. burgdorferi* as compared to the same experiment carried out without fibronectin, which yielded a difference of only 7−11 Ω. This indicates that more target species are attached with the fibronectin present, and this observation agrees with our previous EIS results. It should be noted that the higher value of total impedance of the fibronectin-modified electrode is caused by building-up the layer of insulating species (i.e., bacteria) and thus making the electrode less conducting. Thus, considering that the flow rate was chosen to mimic the flow rate of blood, we have concluded that under these conditions it is possible to identify the bacteria-induced differences in the impedance change at physiological velocities. However, while the 0.06 mL/min flow rate employed here can replicate the tethering (>100 mm/s)[37] of *Borrelia in vivo*, it was not possible to assess this interaction under dragging velocities (<100 mm/s) due to instrumental limitations. The impedance change upon *Borrelia*

exposure at low velocities is highlighted in Figure 8a (inset). It should be noted that impedance values were not observed to always correlate directly with concentration at high concentrations (>1000 cells/ml), despite there always being large impedance changes upon exposure to *B. burgdorferi*; this is likely caused by oversaturation of the electrode surface with large bacterial cells/bacterial fragments, which might lead to competitive attachment effects. In contrast, negligible increase in the total impedance of sensors was observed for both fibronectin-modified (Figure 8c) and bare carbon electrodes (Figure 8d) when exposed to *E. coli*, the species used as our negative control. This set of tests demonstrates that the electrochemical flow-through system can detect specific binding of *Borrelia* species, and possibly recognize the signal variations at velocities corresponding to the forced-induced transient *B. burgdorferi* tethering interactions. To better assess the dragging effects of *B. burgdorferi*, this system will need to be used in conjunction with a more sensitive electrochemical technique such as *in situ*-electrochemical atomic force microscopy or electrochemical quartz crystal microbalance.

Through the above analysis, we have obtained evidence that the BBK32-mediated catch bond mechanism for *B. burgdorferi* can be observed using electrochemical methods utilized in this work; this provides a solid foundation for further development of a flow-mediated functional testing method for *B. burgdorferi*. It is also likely that his methodology can be extended to other pathogenic *Borrelia* species, given their common internal adherence strategy. Finally, given the fact that fibronectin-BBK32/*Borrelia* molecular interactions rely on relatively weak chemical bonding (hydrogen bridging), further electrode modification is required to improve binding specificity and develop a quantitative assay. This is especially true for detection in biological fluids (e.g., blood), where *Borrelia* reside only transiently and in relatively low abundance.

The study demonstrated here has been primarily focused on designing the prototype of an electrochemical flow cell as a tool for the proof-of-concept mimicking the catch-bond mechanism. The next stage of this research will include a series of tests dedicated to specificity of this sensor and the effect of interfering species including *Staphylococcus aureus* and proteins such as collagen, fibrin, and heparan sulfate proteoglycans and their mixture with BBK32 isolate protein and whole *B. burgdorferi* cell extract.

CONCLUSIONS

The goal of the current study was to develop a proof-of-concept electrochemical biosensing approach for *Borrelia*, the Lyme disease-causing bacteria, using a known biological interaction between a bacterial surface protein, BBK32, and the human fibronectin protein. By functionalizing the surface of SPEs with fibronectin, electrodes exhibited a coating of proteins across the entirety of their surface, providing a biomimetic surface that could interact with *B. burgdorferi* in a somewhat specific and sensitive manner. Exposure of the fibronectin-modified electrodes to *B. burgdorferi* produced noticeable changes in impedance, which were not observed with control bacteria, *E. coli*, indicating that specific bacterial adherence to electrodes could be detected. However, given the propensity of fibronectin to bind to many different proteins, a more specific mode of detection was sought. Given the unique catch-bond interaction between BBK32 and fibronectin, one by which tensile force acts to strengthen the observed association, a flow-cell was built and utilized to assess target binding under physiological flow conditions. Using this impedimetric flow cell, impedance changes were observed to change drastically with *B. burgdorferi* exposure, indicating the ability of the apparatus to identify bacterial binding. This additional flow cell component exploits the unique catch-bond behavior of *Borrelia* adherence to distinguish its attachment from other potential adsorbents that cannot withstand the shear flow force.

While the results obtained for the *Borrelia* sensor establish a flow-assisted electrochemical approach, there exist several issues that require improvement for potential diagnostic application. Electrode-to-electrode variation was observed to be relatively high when using commercial SPEs; this led to significantly different initial impedance values that did not necessarily scale with one another. Fabrication of smaller, more precise electrodes (e.g., photolithography) may prove more accurate in future work. For the flow cell measurements, while *B. burgdorferi* exposure always led to a significant increase in impedance, these increases did not always correlate directly with concentration. This inconsistency might be attributed to the large size of the bacterial cell and the high concentrations tested. It will also be beneficial to better optimize the flow-cell injection apparatus in future work to better ensure no external factors are impacting measurements (e.g., bacterial adherence to tubing) and increase sensor sensitivity to better approach biologically relevant levels.

The results presented here represent a proof-of-principle approach for *B. burgdorferi* detection using an electrochemical approach that exploits a unique biological interaction. While the data is promising, there is still much work to be done to achieve a functional electrochemical sensor for the presence of *Borrelia* bacteria as an aid in the diagnosis of Lyme disease. This and other new technologies have the potential to improve the detection of the causative agents of Lyme disease, as well as other infectious diseases, in order to identify diseases earlier and better control disease spread.

ASSOCIATED CONTENT

Supporting Information

The Supporting Information is available free of charge at https://pubs.acs.org/doi/10.1021/acsmeasuresciau.3c00004.

Evolutionary analysis of the BBK32 protein, electrochemical flow cell setup, and surface elemental analysis of oxidized carbon nanotubes and scanning electron microscopy imaging (PDF)

AUTHOR INFORMATION

Corresponding Authors

Connor D. Flynn − Department of Chemistry, Northwestern University, Evanston, Illinois 60208, United States; Department of Chemistry, University of Toronto, Toronto, ON M5S 3G8, Canada; Department of Chemistry, University of New Brunswick, Fredericton, NB E3B 5A3, Canada; orcid.org/0000-0003-0297-0273; Email: connor.flynn@unb.ca

Anna Ignaszak − Department of Chemistry, University of New Brunswick, Fredericton, NB E3B 5A3, Canada; orcid.org/0000-0002-9089-2828; Email: aignasza@unb.ca

Authors

Mariusz Sandomierski − Department of Chemistry, University of New Brunswick, Fredericton, NB E3B 5A3, Canada; Institute of Chemical Technology and Engineering, Poznan University of Technology, 60-965 Poznań, Poland; orcid.org/0000-0001-8227-8062

Kelly Kim − Department of Chemistry, University of New Brunswick, Fredericton, NB E3B 5A3, Canada

Julie Lewis − Department of Biology, Mount Allison University, Sackville, NB E4L 1E2, Canada

Vett Lloyd − Department of Biology, Mount Allison University, Sackville, NB E4L 1E2, Canada

Complete contact information is available at:
https://pubs.acs.org/10.1021/acsmeasuresciau.3c00004

Author Contributions

C.F. and A.I. designed the study and experimental framework. C.F., M.S., K.K., and A.I. conducted the experimental work. V.L. and J.L. provided key reagents and assisted with biological considerations. C.F. and A.I. drafted the manuscript. C.F., A.I., V.L., and J.L. edited the manuscript. CRediT: **Connor D. Flynn** conceptualization (equal), formal analysis (equal), investigation (equal), methodology (equal), writing-original draft (equal), writing-review & editing (equal); **Mariusz Sandomierski** formal analysis (equal), investigation (equal); **Kelly Kim** investigation (supporting); **Julie Lewis** investigation (supporting); **Vett Lloyd** methodology (supporting), resources (supporting), supervision (supporting); **Anna Ignaszak** formal analysis (equal), funding acquisition (equal), investigation (equal), project administration (equal), supervision (equal), visualization (equal), writing-review & editing (equal).

Notes

The authors declare no competing financial interest.

■ REFERENCES

(1) Marques, A. R.; Strle, F.; Wormser, G. P. Comparison of Lyme Disease in the United States and Europe. *Emerg Infect Dis* **2021**, *27*, 2017−2024.

(2) Dong, Y.; et al. Global seroprevalence and sociodemographic characteristics of *Borrelia burgdorferi* sensu lato in human populations: A systematic review and meta-analysis. *BMJ Glob Health* **2022**, *7*, e007744.

(3) Dumic, I.; Severnini, E. 'Ticking Bomb': The impact of climate change on the incidence of Lyme disease. *Canadian Journal of Infectious Diseases and Medical Microbiology* **2018**, *2018*, 1−11.

(4) Zhang, L.; et al. Prevalence and prediction of Lyme disease in Hainan province. *PLoS Negl Trop Dis* **2021**, *15*, e0009158.

(5) Couper, L. I.; MacDonald, A. J.; Mordecai, E. A. Impact of prior and projected climate change on US Lyme disease incidence. *Glob Chang Biol.* **2021**, *27*, 738−754.

(6) Flynn, C.; Ignaszak, A. Lyme disease biosensors: A potential solution to a diagnostic dilemma. *Biosensors* **2020**, *10*, 137.

(7) Piesman, J.; Mather, T. N.; Sinsky, R. J.; Spielman, A. Duration of tick attachment and Borrelia burgdorferi transmission. *J. Clin Microbiol* **1987**, *25*, 557−558.

(8) Guo, B. P.; Norris, S. J.; Rosenberg, L. C.; Hook, M. Adherence of *Borrelia burgdorferi* to the proteoglycan decorin. *Infect. Immun.* **1995**, *63*, 3467−3472.

(9) Probert, W. S.; Kim, J. H.; Höök, M.; Johnson, B. J. B. Mapping the ligand-binding region of *Borrelia burgdorferi* fibronectin-binding protein BBK32. *Infect. Immun.* **2001**, *69*, 4129−4133.

(10) Kim, J. H.; et al. BBK32, a fibronectin binding MSCRAMM from *Borrelia burgdorferi*, contains a disordered region that undergoes a conformational change on ligand binding. *J. Biol. Chem.* **2004**, *279*, 41706−41714.

(11) Pankov, R.; Yamada, K. M. Fibronectin at a glance. *J. Cell Sci.* **2002**, *115*, 3861−3863.

(12) Aguirre, K. M.; McCormick, R. J.; Schwarzbauer, J. E. Fibronectin self-association is mediated by complementary sites within the amino-terminal one-third of the molecule. *J. Biol. Chem.* **1994**, *269*, 27863−27868.

(13) McKeown-Longo, P. J.; Mosher, D. F. Mechanism of formation of disulfide-bonded multimers of plasma fibronectin in cell layers of cultured human fibroblasts. *J. Biol. Chem.* **1984**, *259*, 12210−12215.

(14) Harris, G.; Ma, W.; Maurer, L. M.; Potts, J. R.; Mosher, D. F. *Borrelia burgdorferi* protein BBK32 binds to soluble fibronectin via the N-terminal 70-kDa region, causing fibronectin to undergo conformational extension. *J. Biol. Chem.* **2014**, *289*, 22490−22499.

(15) Schwarz-Linek, U.; et al. Pathogenic bacteria attach to human fibronectin through a tandem β-zipper. *Nature* **2003**, *423*, 177−181.

(16) Arumugam, S.; et al. A multiplexed serologic test for diagnosis of Lyme disease for point-of-care use. *J. Clin Microbiol* **2019**, *57*, e01142-19.

(17) Nayak, S.; et al. Microfluidics-based point-of-care test for serodiagnosis of Lyme disease. *Sci. Rep* **2016**, *6*, 35069.

(18) Kight, E.; et al. Direct Capture and Early Detection of Lyme Disease Spirochete in Skin with a Microneedle Patch. *Biosensors (Basel)* **2022**, *12*, 819.

(19) Garrigues, R. J.; Powell-Pierce, A. D.; Hammel, M.; Skare, J. T.; Garcia, B. L. A structural basis for inhibition of the complement initiator protease Clr by Lyme disease spirochetes. *J. Immunol.* **2021**, *207*, 2856−2867.

(20) Rosca, I. D.; Watari, F.; Uo, M.; Akasaka, T. Oxidation of multiwalled carbon nanotubes by nitric acid. *Carbon N Y* **2005**, *43*, 3124−3131.

(21) Zhong, X.; Qian, G. S.; Xu, J. J.; Chen, H. Y. Cytosensor constructed with a biomimetic fibronectin-functionalized carbon nanotubes on glassy carbon heated electrode. *J. Phys. Chem. C* **2010**, *114*, 19503−19508.

(22) Wang, G.; et al. Variations in Barbour-Stoenner-Kelly culture medium modulate infectivity and pathogenicity of *Borrelia burgdorferi* clinical isolates. *Infect. Immun.* **2004**, *72*, 6702−6706.

(23) Niddam, A. F.; et al. Plasma fibronectin stabilizes *Borrelia burgdorferi*-endothelial interactions under vascular shear stress by a catch-bond mechanism. *Proc. Natl. Acad. Sci. U. S. A.* **2017**, *114*, E3490−E3498.

(24) Klarhöfer, M.; Csapo, B.; Balassy, C.; Szeles, J. C.; Moser, E. High-resolution blood flow velocity measurements in the human finger. *Magn Reson Med.* **2001**, *45*, 716−719.

(25) Vuento, M.; Vartio, T.; Saraste, M.; von Bonsdorff, C.; Vaheri, A. Spontaneous and polyamine-induced formation of filamentous polymers from soluble fibronectin. *Eur. J. Biochem.* **1980**, *105*, 33−42.

(26) Maurer, L. M.; Ma, W.; Mosher, D. F. Dynamic structure of plasma fibronectin. *Crit Rev. Biochem Mol. Biol.* **2016**, *51*, 213−227.

(27) Vartio, T. Disulfide-bonded polymerization of plasma fibronectin in the presence of metal ions. *J. Biol. Chem.* **1986**, *261*, 9433−9437.

(28) Keski-Oja, J. Polymerization of a major surface-associated glycoprotein, fibronectin, in cultured fibroblasts. *FEBS Lett.* **1976**, *71*, 325−329.

(29) Tooney, N. M.; Mosesson, M. W.; Amrani, D. L.; Hainfeld, J. F.; Wall, J. S. Solution and surface effects on plasma fibronectin structure. *J. Cell Biol.* **1983**, *97*, 1686−1692.

(30) Miklossy, J.; et al. Persisting atypical and cystic forms of *Borrelia burgdorferi* and local inflammation in Lyme neuroborreliosis. *J. Neuroinflammation* **2008**, *5*, 40.

(31) Margulis, L.; et al. Spirochete round bodies Syphilis, Lyme disease & AIDS: Resurgence of 'the great imitator'? *Symbiosis* **2009**, *47*, 51−58.

(32) Brorson, Ø.; et al. Destruction of spirochete *Borrelia burgdorferi* round-body propagules (RBs) by the antibiotic Tigecycline. *Proc. Natl. Acad. Sci. U. S. A.* **2009**, *106*, 18656−18661.

(33) Rudenko, N.; Golovchenko, M.; Kybicova, K.; Vancova, M. Metamorphoses of Lyme disease spirochetes: Phenomenon of Borrelia persisters. *Parasit Vectors* **2019**, *12*, 237.

(34) Feng, J.; Auwaerter, P. G.; Zhang, Y. Drug combinations against *Borrelia burgdorferi* persisters in vitro: Eradication achieved by using daptomycin, cefoperazone and doxycycline. *PLoS One* **2015**, *10*, e0117207.

(35) Gaultney, R. A.; Gonzalez, T.; Floden, A. M.; Brissette, C. A. BB0347, from the Lyme disease spirochete *Borrelia burgdorferi*, is surface exposed and interacts with the CS1 heparin-binding domain of human fibronectin. *PLoS One* **2013**, *8*, e75643.

(36) Brissette, C. A.; et al. The borrelial fibronectin-binding protein RevA is an early antigen of human Lyme disease. *Clinical and Vaccine Immunology* **2010**, *17*, 274−280.

(37) Ebady, R.; et al. Biomechanics of Borrelia burgdorferi Vascular Interactions. *Cell Rep* **2016**, *16*, 2593−2604.